Korean Chem. Eng. Res., 56(2), 269-274 (2018)
https://doi.org/10.9713/kcer.2018.56.2.269
PISSN 0304-128X, EISSN 2233-9558

Effect of Cerium loading on Stability of Ni-bimetallic/ZrO_2 Mixed Oxide Catalysts for CO Methanation to Produce Natural Gas

Annabathini Geetha Bhavani*,† and Hyunki Youn**

*Department of Chemistry, School of Science, Noida International University, Gautam Budh Nagar, Uttar Pradesh 203201, India
**University-Industry Cooperation Foundation, Chungbuk National University, 1, Chungdae-ro, Seowon-Gu, Cheongju, Chungbuk, 28644, Korea

(Received 13 July 2017; Received in revised form 6 October 2017; accepted 25 October 2017)

Abstract – All the Ni-Co-Ce-ZrO_2 mixed oxides are prepared by co-precipitations methods. Methanation of CO and H_2 reaction is screened tested over different fractions of cerium (2, 4, 7 and 12 wt.%) over Ni-Co/ZrO_2 bimetallic catalysts are investigated. The mixed oxides are characterized by XRD, CO-Chemisorption, TGA and screened methanation of CO and H_2 at 360 °C for 3000 min on stream at typical ratio CO:H_2=1:1. In Ni-Co/CeZrO_2 series 2 wt.% Ce loading catalyst shows most promising catalyst for CH_4 selectivity than CO_2, which directs more stability with less coke formation. The high activity is attributed to the better bimetallic synergy and the well-developed crystalline phases of NiO, ZrO_2 and Ce-ZrO_2. Other bimetallic mixed oxides NCoZ, NCo$C^{4\text{-}12}$Z has faster deactivation with low methanation activity. Finally, 2 wt.% Ce loading catalyst was found to be optimal coke resistant catalyst.

Key words: Cerium, NiO, ZrO_2, Bimetallic mixed oxide catalysts, Methanation

1. Introduction

Methanation has received considerable attention as an efficient method of producing natural gas substitute which involves the partial oxidation of coal to CO and H_2 followed by the recombination of these gases to form methane. A number of reports have been published on the synthesis and characterization of Ni-based methanation catalysts [1]. The formation of nickel carbide during reaction and the coke deposition were observed on these catalysts, as a consequence, their industrial use is improbable.

The main challenge for methanation seems to be the development of highly active catalysts with a high resistance to coke deposition at CO:H_2 mole ratio of 1:1. It has been shown that cerium oxides and cobalt oxides can play an important role in oxidation reaction. CeO_2 is an important component in the three-way catalyst [2]. The main properties of cerium oxides for this three-way catalyst (TWC) application are (i) a large oxygen storage capacity via the redox process Ce^{4+} to Ce^{3+}; (ii) improvement of the dispersion of noble metals; (iii) improvement of the thermal stability of supports; and (iv) promotion of the water–gas shift reaction. Cobalt-based oxides are the good candidate catalysts for diesel soot combustion [3]. Co_3O_4 shows highly catalytic activity for the combustion of CO and organic compounds. The activity and selectivity of such catalysts are related to the strong redox ability of CoOx. Despite the fact that CeO_2 and Co_3O_4 catalysts have been extensively studied for oxidation reaction and TWC application, few detailed studies have analyzed the utilization of CeO_2-supported cobalt oxide materials for soot combustion. Harrison et al. [4] sightsaw the CoO/CeO_2 catalytic system for soot oxidation. It is clear that bimetallic catalysts may exhibit superior performance for methane production compared with the corresponding monometallic catalysts. Ce-ZrO_2 systems have been intensively developed as automotive exhaust catalysts over last decades [5].

In this study promoters were screened since it proven to suppress carbon formation [6]. Ruckenstein et al. [7], reported that lower metal loading catalysts had better carbon resistance by improving CO oxidation. New catalyst formulations are being developed by addition of promoters Fe [8], Ce [9], Co, Ni [10,11] that enhance oxygen adsorption for coke-resistant catalyst. Copper catalysts on alternative supports such as ceria, or other ceria-promoted supports are also being developed in an attempt to provide selective surface oxygen for CO oxidation at low temperatures [12]. Therefore, our study was devoted to CO methanation over Ni-bimetallic Zr-supported catalysts were prepared by co-precipitation method, in order to evaluate the effect of ceria addition and loading over the NiCoZr denoted as a NCZ. Amount of cerium loading varied NiCoCe*Zr with *2, 4, 7 and 12 wt% were carefully examined for CO methanation at 360 °C at CO:H_2 typical mole ratio of 1:1.

All bimetallic mixed oxides were characterized by X-ray diffraction (XRD), surface area with BET, elemental analysis, coke morphology by SEM analysis and total amount by thermal gravimetric analysis (TGA) are presented.

2. Experimental

2-1. Catalyst preparation

Zirconium-supported Ni-bimetallic catalyst was prepared by co-

† To whom correspondence should be addressed.
E-mail: geetha.bhavani@niu.edu.in

precipitating a common aqueous solution of nickel nitrate (98% purity; Lancaster Synthesis), cerium nitrate (Kanto chemicals co Inc), cobalt nitrate (99% purity; Aldrich) respectively. The salt nitrates were precipitated with NaOH solution, respectively. The precipitate cake was washed using deionized water 2 or 3 times, dried overnight in the air at 120 °C, and then calcined in the air at 600 °C for 3 h. Different cerium content 2, 4, 7 and 12 wt% over Ni-Co-Ce-Zr-O were designated as NCoC*Z (C*=C^2, C^4, C^7 and C^{12}) respectively.

2-2. Catalyst characterization

The crystal structures of calcined alloy samples were determined by XRD measurement on an X'pert pro rotator diffractometer operation at 30 mA and 45V using Co Kα as radiation source (λ=0.1790). The data of 2θ from 10~80° were collected. Surface area, pore volume and pore size distribution were measured by nitrogen adsorption/desorption at 77 K using a Quadrasorb SI instrument. The samples were degassed at 350 °C for 10 h prior to the adsorption experiments. The surface area (S_{BET}) was determined by BET method in 0~0.3 partial pressure range and the pore size distribution was determined by Barrett-Joyner-Halenda (BJH) method from the desorption branch of isotherm. For CO pulse chemisorptions the sample was purged in the helium flow until a constant baseline level was attained. In pretreatment, clean surface of metal is exposed by oxidation at 550 °C for 4 h in O_2 flow followed by reduction at 550 °C for 2 h in H_2 flow. Chemisorptions were carried out with CO flow at 35 °C for 30 min, and desorption was carried out with a linear heating rate (10 °C/min) in a flow of He (20 ml/min). Metal dispersion percentage and total metal surface area were calculated assuming a CO molecule titrates one exposed metal atom. TGA was conducted on thermogravimeter (Mettler Toledo, TG-SDTA 851 instrument) using air as a carrier gas and with a heating rate of 10 min^{-1}. Prior to each TGA experiment, all samples were stored over anhydrous $CaCl_2$ in a desiccator for at least 24 h to ensure a complete sample hydration. The thermograms so obtained provide valuable information about the relative amount of coke constituents present in the sample. Scanning electron microscopy (SEM) analysis of calcined and used catalyst to see the coke morphology was examined by a JEOL JSM 6400 scanning electron microscope.

2-3. Catalytic activity

Catalytic tests were carried out in a tubular fixed-bed flow reactor at atmospheric pressure. 0.3 g of catalyst was loaded prior to reduction treatment. Catalyst bed was preheated at 530 °C for 30 min, and reduced in flowing H_2 at 530 °C for 2 h. The reactions were performed at atmospheric pressure at 360 °C using a mixture of carbon monoxide and hydrogen at a ratio of CO:H_2=1:1 balance, which was diluted with N_2. The gas hourly space velocity (GHSV) was 21000^{-1}. The product gas stream was analyzed by online gas chromatography (Agilent Inc.) with a 60/80 carboxen EN 1000 molecular sieve column. To determine conversion and selectivity, the products were collected after 30 min of steady-state operation. The conversions of carbon monoxide and hydrogen were determined from the ratios of the difference in the molar flow rates in the feed minus the product to the feed molar flow rate. The molar flow rates were assumed proportional to their concentration in the gas streams. Selectivities were calculated as moles of individual products produced per mole of total products (methane plus carbon dioxide) produced.

3. Result and Discussion

3-1. Catalysts surface properties

The catalyst compositions and BET surface areas are listed in Table 1. The surface areas of $NCoC^2Z$, $NCoC^4Z$, $NCoC^7Z$, $NCoC^{12}Z$ catalysts spectacles 52.4, 47.4, 41.2 and 29.6 m^2/g, respectively. The surface area of NCoZ (without Ce loading) is 24.5 m^2/g. 2 wt% of Ce loading over NCoZ catalyst show tremendous increase in surface area upto 52.4 m^2/g. It was perceived from catalysts series $NCoC^{2\text{-}7}Z$ the surface areas are decreased with increasing the cerium loading and shows maximum over $NCoC^2Z$ catalyst. Surface area of catalyst has directly influence the metal dispersion, which is well identified in Table 2 by CO pulse chemisorption. $NCoC^2Z$ catalyst show highest metal dispersion of 7.9% with metallic Ni surface area of 2.8 m^2/g compared to with and without Ce fractions. Our earlier report bared that $Ni/CoMnZrO_2$ trimetallic catalyst improves the surface area by threshold addition of Ce fractions as a promoter, which endow well dispersed Ni and Co nano sized particles to improve the autothermal CO_2 reforming with methane by providing the surface oxygen to oxidize the coke [13].

XRD diffractograms of the entire mixed oxide catalysts after calcination of 600 °C for 3 h are shown in Fig. 1. XRD patterns in Fig. 1 (bimetallic mixed oxide catalysts with ceria and without ceria) shows polycrystalline phases, such as ZrO_2, NiO and $CeZrO_2$ without separated CeO_2 or any other impurity phases, which indicates good catalysts. Main broad diffraction lines are due to a cubic fluorite type phase

Table 1. Physio-chemical properties of Ni-bimetallic/ZrO_2 mixed oxide catalysts

Catalyst code[a]	Metal content wt%				Surface area m^2/g	Elemental analysis %			
	Ni	2nd metal	Ce	Zr		Ni	2nd metal	Ce	Zr
NCoZ	20	10	0	70	24.51	19.9	9.7	0	69.94
$NCoC^{2*}Z$	20	10	2	68	52.49	19.97	9.9	1.98	67.98
$NCoC^{4*}Z$	20	10	4	66	47.45	19.94	9.8	3.97	65.95
$NCoC^{7*}Z$	20	10	7	63	41.27	19.89	9.8	6.91	62.96
$NCoC^{12*}Z$	20	10	12	58	29.65	19.9	9.7	11.87	57.89

[a]Prepared by co-precipitation method.
*$C^{2\text{-}12}$ varying cerium loading of 2, 4, 7 and 12 wt%

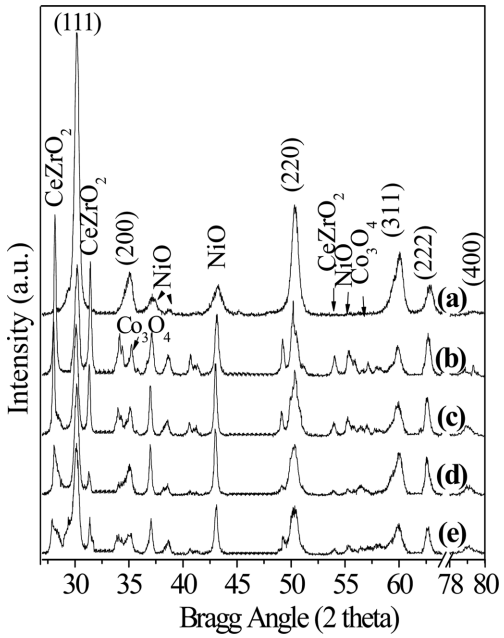

Fig. 1. XRD patterns of different cerium loadings over (a) NCoZ, (b) $NCoC^2Z$, (c) $NCoC^4Z$, (d) $NCoC^7Z$ and (e) $NCoC^{12}Z$ catalysts after 600 °C of calcination.

corresponding to (111), (200), (220), (311), (222) and (400) planes of ZrO_2 supports (PDF-ICDD 28-0271). Hence this indicates that CeO_2 is totally incorporated into the ZrO_2 lattice to form a homogeneous solid solution. Compared to NCoZ, cerium loaded $NCoC^{2\text{-}12}Z$ catalysts shows intense reflections of $CeZrO_2$ phase at 30.97° and small reflections at 49.8°, 58.6° of monoclinic phase. $CeZrO_2$ phase reflections at 29°, 30.97° over $NCoC^2Z$ catalyst are sharper, but further increasing the cerium loading these reflections were decreased and became broad, and all the NiO and ZrO_2 reflection were decreased, which clearly indicates that further cerium loading may affect the crystallinity and bimetallic synergic properties. Fig. 1b show spinal Co_3O_4 phase, with addition of Ce as a promoter and intensity decreases with increasing Ce loading, which served as an active site on the surface. Similar observation was made by Ocampo et al. [14] over $CeZrO_2$ by inserting the transitional metals of Fe^{3+} and Co^{2+} mixed oxides over methanation of CO_2.

Pattern of $NCoC^7Z$ and $NCoC^{12}Z$ in Fig. 1 shows strong reflection of NiO and ZrO_2, a two small peaks at 28°, 30.97° indicate cerium is partially present in $CeZrO_2$ phase on the surface of the catalyst and low intensity of peaks. $NCoC^2Z$ diffractogram shows well prominent peaks of NiO, ZrO_2 and $CeZrO_2$ indicates high crystallinity with high surface area. An interesting note is mixed alloy systems $NCoC^2Z$ are shown similarity in XRD reflections except for spinal Co_3O_4 phase. Recently Liang et al. [15] and Reddy et al. [16] also reported similar rich crystalline phase over copper-doped ceria-zirconia mixed oxides. It is noteworthy that optimal loading of cerium (2 wt%) over Ni-Co/ZrO_2 mixed oxides reflects high crystallinity with prominent crystalline phases of NiO, ZrO_2 and $CeZrO_2$ were well identified. Elemental analysis of the catalysts are shown in Table 1 are well agreement with initial salt solution.

3-2. Effect of cerium loading over NCoZ catalyst on stability

Fig. 2a shows the conversion of CO over Ni-Co/ZrO_2 mixed oxides catalysts with and without cerium loading at 360 °C for 3000 min on stream. Among all the catalysts $NCoC^2Z$ shows high conversion at initial 86.7 to 92.5% at 3000 min and maintains steady state. NCoZ (without cerium) catalyst shows initial conversion of 84.1% and stable up to 1600 min with 80.5% conversion. Other cerium-varied catalysts $NCoC^4Z$ and $NCoC^7Z$ show similar stability and conversion of 62.1%. Only low cerium addition may alter the catalyst structure for suitable methanation catalysts due to its unique redox property and high oxygen storage capacity [17]. It clearly indicates that catalysts activity in soot combustion mainly depends on the mobility of oxygen on catalyst that can offer more active oxygen at reaction temperature [18]. Fig. 2b-c shows selectivity of CO_2 and

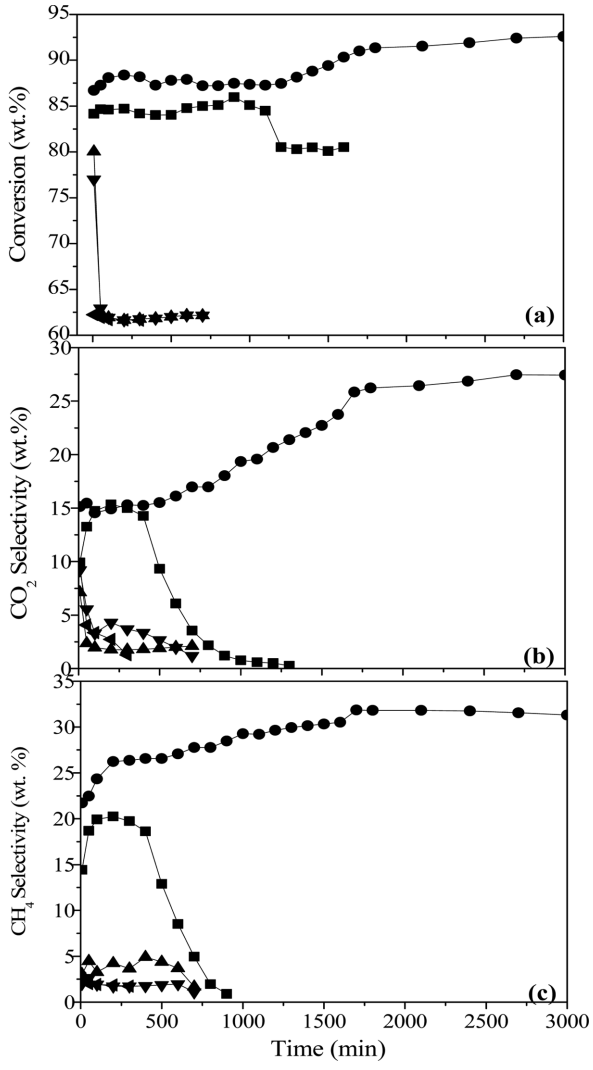

Fig. 2. (a-c) Catalytic activity of varying cerium content 2, 4, 7 and 12 wt% over Ni-Co/ZrO_2 oxide catalyst at 360 °C for 3000 min on stream methanation, (a) conversion of CO, (b) CO_2 selectivity, (C) CH_4 selectivity over (●) $NCoC^2Z$, (■) NCoZ, (▲) $NCoC^4Z$, (◄) $NCoC^7Z$ and (▼) $NCoC^{12}Z$ catalysts.

CH_4 over NCoZ, initial 9.92 and 14.43 at final 0.2 and 0.9 and stable up to 1300 min. 2 wt% cerium loading over NCoZ ($NCoC^2Z$) catalyst show remarkable activity for methanation in presence of H_2, and NCoZ and $NCoC^{4\text{-}12}Z$ catalysts (Ce content 4, 7 and 12 wt%) were relatively inactive in terms of selectivity and stability. However, $NCoC^2Z$ catalyst shows highest selectivity of CO_2 and CH_4 initially 15.4 and 21.7 wt% and finally 27.4 and 31.3 wt% in steady state until 3000 min on stream. High dispersion and metallic surface area, crystallinity play a major role in enhancing the performance of the catalyst. Meanwhile, the addition of Ce also played a promoter role in the enhancement of physical and chemisorption properties [13,19] of the catalyst which probably affected the physical structure by making it less crystalline and also contributes in the CO conversion mechanism to form methane. $NCoC^{12}Z$ catalyst shows less selectivity of CO_2 and CH_4, 9.7 and 2.5 wt% respectively and unstable after 300 min on stream. At higher cerium concentration decreases the metal dispersion which leads to deactivation significantly. This may be probably due to the blocking of external surface of the catalyst by large metals aggregates, which was confirmed by significant decrease of BET surface area for the catalyst with cerium loading 2 to 12 wt%. TGA results from Table 1 show the least coke formation over $NCoC^2Z$ catalyst, methanation proceeds after 3000 min, which confirms its high stability. Cerium may undergo changes in the oxygen chemical potential allowing these materials to act as very effective oxygen buffers during the reaction, which will affect the bimetallic synergy in promising way [20]. Increasing the cerium loading to 4 to 12 wt%, deactivation is more and coke formations keep around 1.90 to 7.01 wt%, respectively. NCoZ catalyst shows the highest coke formation of 8.68 wt% among Ni-Co catalytic systems.

However, doping of ceria with aliovalent cations, probably introduced into the network of the fluorite type oxide, has been an efficient way to generate oxygen vacancies, permitting a high mobility of oxygen from bulk to surface. Ability of mobility of oxygen from bulk to surface play a significant role in oxidation of surface carbon formed, which active sites are accessible for further methanation reaction. In addition, the doping of ceria positively influences the thermal stability and the surface area of the compound in comparison to the pure oxides [7]. From the XRD pattern of the $NCoC^4Z$, $NCoC^7Z$ and $NCoC^{12}Z$ catalysts, it is observed that the entire 2θ angle corresponding Ce-ZrO_2 and NiO reflections were decreased with increasing the cerium loading, which may affect the crystallinity and bimetallic synergy between support and metals in terms of stability. Even BET surface areas from Table 1 show that surface areas decrease from 52.49 to 29.65 m^2/g with cerium increase from 2 to 12 wt%. This indicates no adhesion of carbon species to the catalysts surface and to their loose structure, which does not hamper diffusion of the products (CO_2 and CH_4) gases over catalyst surface, which leads to the catalyst deactivation via fouling. Even metallic surface area of $NCoC^{12}Z$ catalyst 0.1 m^2/g indicates less dispersion of metals with 7.01% of coke formation. Finally, high methanation activity over $NCoC^2Z$ and $NCoC^{12}Z$ catalysts may be due to Co, Ce (2 wt%) and Ni metals capable to grab the surface carbon converting into building units of the hydrocarbon chain growth process. This also indicates the higher surface area leads to more metals dispersion with high stability of the catalysts. $NCoC^2Z$ catalyst is screened to be best candidate in stability and conversion of the Ni-Co catalytic systems are as follows: $NCoC^2Z$ <NCoZ <$NCoC^4Z$ <$NCoC^7Z$ <$NCoC^{12}Z$ catalysts.

On the other hand, Uner et al. [21] reported that the pronounced activity of cobalt oxide catalysts seems due to the surface oxygen coming after reduction process of the oxide itself. In the presence of another reducible oxide such as CeO_2, the oxygen needed for the oxidation reaction would be provided by the second oxide. A spillover mechanism at the cobalt oxide-ceria interface is postulated to be the main mechanism for soot oxidation. Moreover, the high oxygen mobility offered the other advantage of reducing the CO formation from the soot combustion. Therefore, these mixed oxides with high oxygen mobility may be very important in soot oxidation reactions to maintained stability. The best catalytic activity of $NCoC^2Z$ catalyst may be due to better bimetallic synergy between metals. It is noteworthy that threshold factions of alloys were previously found to be high catalytic activity for partial oxidation of methane to syngas [22]. $NCoC^2Z$ catalyst have shown stable performance, it seems that carbon formation over all the catalysts has a very clear relationship with time on stream (TOS). Carbon accumulation becomes significantly slower with increasing TOS. From TGA results and overall activity of Table 1, it is speculated that rapid carbon formation during the few hours slowed additional carbon formation, through which stable performance is followed. Similar observation was made by Zhang et al. [23] and Kramer et al. [1] over Ni based catalyst for methanation. So, this catalysts can be promising to be the most stable that ever been developed for syngas of CH_4 production at typical ratio $CO:H_2$ mole ratio of 1:1. These results represent in above catalysts systems and reaction conditions studied are distinguished by following equations:

$$CO_g + 2s \leftrightarrow CO_a \quad (1)$$
$$CO_a \leftrightarrow C_a + O_a \quad (2)$$
$$H_{2\,g} + 2s \leftrightarrow 2H_a \quad (3)$$
$$O_a + H_a \leftrightarrow OH_a + s \quad (4)$$
$$OH_a + H_a \rightarrow H_2O_g \quad (5)$$
$$C_a + H_a \leftrightarrow CH_a + s \quad (6)$$
$$CH_a + H_a \leftrightarrow CH_{2\,a} + s \quad (7)$$
$$CH_{2\,a} + H_a \leftrightarrow CH_{3\,a} + s \quad (8)$$
$$CH_{3\,a} + H_a \rightarrow CH_{4\,g} \quad (9)$$

Here, **s** represents a free surface site and subscripts **a** and **g** represent adsorbed and gas-phase species, respectively. It is assumed that CO adsorbs on two sites prior to dissociation on the same sites and that hydrogen competes for the same sites. It is assumed that all steps prior to the rate-determining steps are in equilibrium. The assumption that eq. (5) is not in equilibrium would appear different from Van Meerten et al. [24], who considered a series of different equations which they then attempt to fit to their data. They showed that the

Table 2. Chemisorption properties of Ni-bimetallic/ZrO_2 mixed oxide catalysts

Catalyst code	Metal dispersion (%)[b]	Metallic surface area m^2/g[b]	Coke content wt%[c]
NCoZ	0.4	0.1	8.68
$NCoC^{2*}Z$	7.9	2.8	0.78
$NCoC^{4*}Z$	4.3	1.4	1.90
$NCoC^{7*}Z$	1.9	0.5	3.94
$NCoC^{12*}Z$	0.5	0.1	7.01

[b]Measured from Auto Chem program in CO pulse chemisorptions.
[c]coke content is measured after 3000 min of methanation by TGA analysis.

best fit to their data was obtained if the rate determining step was the combination of CH_a and H_a species [eq. (7)], concurrently with desorption of water [eq. (5)]. These mechanism steps which described the experimental data were based on dissociative adsorption of carbon monoxide and addition of a hydrogen atom to adsorbed CH_x as the rate determining step. The results are consistent with the conclusions discussed above.

3-3. Coke formation over various Cerium loading factions

The coke formation is evident from the XRD spectra, SEM analysis and TGA analysis shown in Table 2. XRD pattern of spent catalysts in Fig. 3 is a good agreement of coke yield over $NCoC^2Z$, and NCoZ (without cerium) catalysts. It was clear that the crystallite of zirconia in the tetragonal phase at 2θ around 30° and graphitic carbon were observed after the catalysts were exposed to the methanation at 360 °C for 3000 min on stream.

As discussed earlier, zirconia could be in the form of well-dispersed, composite forms. Under the temperature and long term reaction atmosphere, the well-dispersed and amorphous forms could be

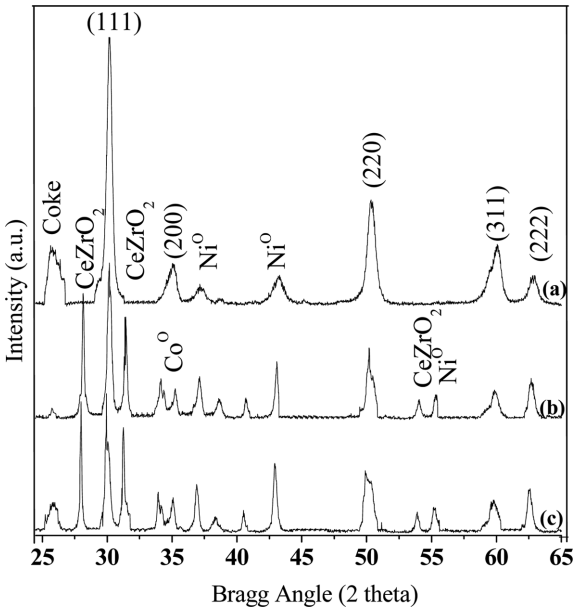

Fig. 3. XRD patterns of spent catalysts of (a) NCoZ, (b) $NCoC^2Z$ and (c) $NCoC^{12}Z$ catalysts after methanation of CO of 3000 min on stream.

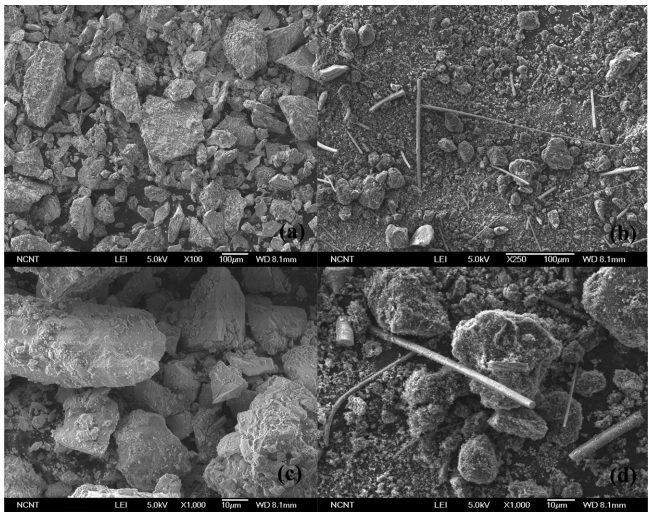

Fig. 4. SEM images of (a) fresh catalyst-NCoC2Z, (b) Spent catalyst-NCoC2Z, (c) fresh catalyst-NCoZ (without cerium) and (d) Spent catalyst-NCoZ (without cerium) are evident after 3000 min on stream.

transformed to tetragonal ZrO_2. It strongly speculated that the coke reduction could be promoted by ZrO_2 in the presence of $CeZrO_2$ on $NCoC^2Z$, thus enhancing CO dissociation and oxidation of coke. Further, the rate determining step is formation of adsorbed carbon and oxygen on the surface. This causes gasification of the dissociated oxygen and unsaturated intermediates and prevents the formation of carbon deposit precursors in the system. From Fig. 4(b and d) the formation of carbon filaments and amorphous carbon in SEM images are clearly evident after 3000 min on stream, and activity is in good agreement with TGA results (Table 2). As shown in figure (Fig. 4b and d) a number of nodes studded in the filamentous coke were procured from surface. It had a considerably rough surface where coke (graphite) aligned perpendicular to the base metal. Finally it's noteworthy that coke formation is in considerable amounts over $NCoC^2Z$, it may be due to Co and Ce metal, which forms better coke-oxidative synergy with $CeZrO_2$ support that make stable conversion and selectivity for long time on stream. The key for improving CO oxidation is to add sites for oxygen adsorption to have a noncompetitive dual-site mechanism for CO oxidation. The new bimetallic NCoCZ catalyst is being developed by addition of Ce as a promoter in all the catalyst systems that enhance oxygen adsorption.

4. Conclusion

Comprehensive information about cerium role and influence of second metal for catalyst stability on methanation was suggested. It was concluded that 2 wt% cerium have high stability towards coke formation probably due to better bimetallic synergy. Ni-Co/$CeZrO_2$ catalyst show high catalytic activity with stability, capability to oxidize the surface carbon and converted hydrocarbon chain process to formation of methane. Oxidation of surface carbon helps to accessible further methanation on surface active sites. Bimetallic mixed

oxide catalysts give further understanding of the modes of deactivation and coking during catalytic conversions of CO and H_2 to produce methane. The results of this work suggest that it is possible to increase substantially the efficiency of Ni-bimetallic methanation catalyst by alloying with Ce and Co to lower the catalyst cost.

Acknowledgements

We gratefully acknowledge for financial support to RIST, Pohang, South Korea.

References

1. Krämer, M., Stöwe, K., Duisberg, M., Müller, F., Reiser, M., Sticher, S. and Maier, W. F., *Appl. Catal. A: Gen*., **369**, 42-52 (2009).
2. Sayle, D. C., Maicaneanu, S. A., Watson, G. W., *J. Amer. Chem. Soc*., **124**, 11429-11439 (2002).
3. Liu, J., Zhao, Z., Wang, J., Xu, C., Duan, A., Jiang, G., Yang, Q., *Appl. Catal. B: Envir*., **84**, 185-195(2008).
4. Harrison, P. G., Ball, I. K., Daniell, W., Lukinskas, P., Céspedes, M., Miró, E. E. and Ulla, M. A., *Chem. Eng. J.*, **95**, 47-55(2003).
5. Fornasiero, P., Balducci, G., Kaspar, J., Meriani, S., di Monte, R. and Graziani, M., *Catal. Today*, **29**, 47-52(1996).
6. Seok, S. H., Choi, S. H., Park, E. D., Han, S. H., Lee, J. S., *J. Catal*., **209**, 6-15(2002).
7. Ruckenstein, E. and Hu, Y. H., *J. Catal.*, **162**, 230-238(1996).
8. Watanabe, M., Uchida, H., Ohkubo, K., Igarashi, H., *Appl. Catal. B: Envir.*, **46**, 595-600(2003).
9. Monte, R. D. and Kašpar, J., *Topics Catal*., **28**, 47-57(2004).
10. Suh, D. J., Kwak, C., Kim, J. H., Kwon, S. M. and Park, T. J., *J. Power Sources*, **142**, 70-74(2005).
11. Ko, E. Y., Park, E. D., Seo, K. W., Lee, H. C., Lee, D. and Kim, S., *Catal. Letters*, **110**, 275-279(2006).
12. Avgouropoulos, G., Ioannides, T., Papadopoulou, Ch., Batista, J., Hocevar, S. and Matralis, H. K., *Catal. Today*, **75**, 157-167(2002).
13. Bhavani, A. G., Kim, W. Y., Kim, J. Y., Lee, J. S., *Appl. Catal. A: Gen*., **450**, 63-72(2013).
14. Ocampo, F., Louis, B. and Roger, A., *Appl. Catal. A: Gen*., **369**, 90-96(2009).
15. Liang, Q., Wu, X. D., Weng, D. and Lu, Z. X., *Catal. Comm*., **9**, 202-206(2008).
16. Reddy, B. M. and Rao, K. N., *Catal. Comm*., **10**, 1350-1353(2009).
17. Bueno-López, A., Krishna, K., Makkee, M., and Moulijn, J. A., *J. Catal*., **230**, 237-248(2005).
18. Shumin, S., Wenling, C. and Weishen, Y., *Chinese J. Catal*., **30**, 685-689(2009).
19. Leitenburg, C., Trovarelli, A. and Kašpar, J., *J. Catal*., **166**, 98-107(1997).
20. Park, S., Vohs, J. M. and Gorte, R. J., *Nature*, **404**, 265-267(2000).
21. Uner, D., Demirkol, M. K. and Dernaika, B., *Appl. Catal. B: Envir*., **61**, 334-345(2005).
22. Kustov, A. L., Frey, A. M., Larsen, K. E., Johannessen, T., Nørskov, J. K. and Christensen, C. H., *Appl. Catal. A: Gen*., **320**, 98-104 (2007).
23. Zhang, J., Wang, H. and Dalai, A. K., *J. Catal*., **249**, 300-310(2007).
24. van Meerten, R. Z. C., Vollenbroek, J. C., de Croon, M. H. J. M., van Nisselrooij, P. F. M. T. and Coenen, J. W. E., *Appl. Catal*., **3**, 29-56(1982).